

A Journal of the Gesellschaft Deutscher Chemiker

Angewandte Chemie

GDCh

International Edition

www.angewandte.org

Accepted Article

Title: A Phenomenological Symmetry Rule for Chemical Reactivity under Vibrational Strong Coupling

Authors: Anjali Jayachandran, Bianca Patrahau, John G. Ricca, Malay Mahato, Y. Pang, Kalaivanan Nagarajan, Anoop Thomas, Cyriaque Genet, and Thomas W. Ebbesen

This manuscript has been accepted after peer review and appears as an Accepted Article online prior to editing, proofing, and formal publication of the final Version of Record (VoR). The VoR will be published online in Early View as soon as possible and may be different to this Accepted Article as a result of editing. Readers should obtain the VoR from the journal website shown below when it is published to ensure accuracy of information. The authors are responsible for the content of this Accepted Article.

To be cited as: *Angew. Chem. Int. Ed.* **2025**, e202503915

Link to VoR: <https://doi.org/10.1002/anie.202503915>

A Phenomenological Symmetry Rule for Chemical Reactivity under Vibrational Strong Coupling

A. Jayachandran, B. Patrahau, J.G. Ricca, M. Mahato, Y. Pang¹, K. Nagarajan², A. Thomas³, C. Genet, T.W. Ebbesen**

University of Strasbourg, CNRS, ISIS & icFRC,
8 allée G. Monge, 67000 Strasbourg, France.

Current addresses:

¹School of Science, Shandong Jianzhu University, Jinan 250101, Shandong, China.

²Department of Chemical Sciences, Tata Institute of Fundamental Research, Mumbai 400005, India

³Department of Inorganic and Physical Chemistry, Indian Institute of Science, Bengaluru - 560 012, India

Abstract

Symmetry is known to strongly influence the course of a chemical reaction. It has also been found to play a key role in vibrational strong coupling (VSC), where it can influence the outcome of chemical reactions or alter chemical equilibria. However, the precise nature of this effect and its extent remains elusive. To further explore the role of vibrational symmetry, we have investigated the equilibrium constants of different charge transfer complexes, in particular of isomers of trimethyl benzene belonging to different point groups from which a general symmetry rule emerges. We describe the strongly coupled system by a direct product of irreducible representations associated with the complexes and the cavity. As a consequence, the coupled vibration is associated with a new irreducible representation that projects differently on the reaction coordinate of the charge transfer complexation, reflecting the changes in the equilibrium constants. This phenomenological symmetry rule points to a general underlying framework for predicting the outcome of chemical reactivity under VSC.

Key words: Symmetry, vibrations, strong coupling, charge transfer, rule

Introduction:

The role of symmetry in chemical reactivity has long been of interest to chemists, most notably as illustrated by the Woodward - Hoffman rules which predict the outcome of pericyclic reactions and correlate the molecular orbital symmetry of the reactant with that of the product.^[1] The symmetry of a molecule, given by its corresponding point group, affects spectroscopic selection rules, thermodynamic properties and determines the irreducible representations of its vibrations.^[2-8] Molecular vibrations are crucial in the course of a chemical reaction and its dynamics.^[6-16] And as pointed out by Bader over 60 years ago, the symmetry correlation between the vibrations and the electronic manifold strongly affects the outcome of reactions.^[6]

Symmetry also plays a critical role in vibrational strong coupling (VSC), a new frontier of research where much remains to be understood.^[17-54] In VSC, the electromagnetic fluctuations of an optical resonance, its zero-point energy, is coupled to a given vibrational band of a molecule. As a consequence it occurs in the dark and no external photons are injected inside the cavity. Typically, the molecular vibration of N identical molecules is coupled to a single optical mode of a cavity which gives rise to two bright light-matter hybrid vibro-polaritonic states, VP^+ and VP^- , and $N-1$ dark states (DS) as illustrated in Fig 1. The strength of this collective coupling is directly proportional to the transition dipole moment of the coupled vibration and \sqrt{N} .^[19-20] To achieve the strong coupling regime, the energy splitting between VP^+ and VP^- , known as the Rabi splitting energy, must be larger than the full-width-half-maximum of the vibrational band and the cavity mode. In other words, the coupling strength must overcome the dissipative processes. VSC can be achieved by direct coupling of the solute or the solvent, or alternatively, the solute can be coupled by cooperative coupling through a vibrational band of the solvent that overlaps with the vibrational band of the solute.^[20]

One of the surprising features of the VSC is that it can lead to very large changes in chemical rates, thermodynamics and product ratios even though the collective Rabi splitting is only $\sim k_B T$ and the chemical event occurs at the molecular level. Thus, the energy perturbation induced by the Rabi splitting is not responsible for the VSC induced effects. In all these experiments, the resonant nature of VSC is a crucial aspect. First, it provides a unique way to access, by the choice of the vibration, an on-site selectivity of chemical reactions under VSC.^{[17-}

22, 31-33] Then, as we found serendipitously, symmetry plays a fundamental role in the change in chemical reactivity induced by VSC. [17] This finding was possible precisely because VSC allows for selective coupling of molecular vibrations of a given symmetry. We exploited this unique feature in the context of the charge transfer complexation of mesitylene- I_2 and benzene- I_2 and observed that the modification of the equilibrium constant depends *only* on the symmetry of the vibrational mode of the molecule resonantly coupled to the cavity mode. The type of vibration (e.g. bending, stretching, etc.) and their energy had little if any influence. From this resonant symmetry selection, we further demonstrated that VSC can influence the stereoselectivity of pericyclic reactions. [18]

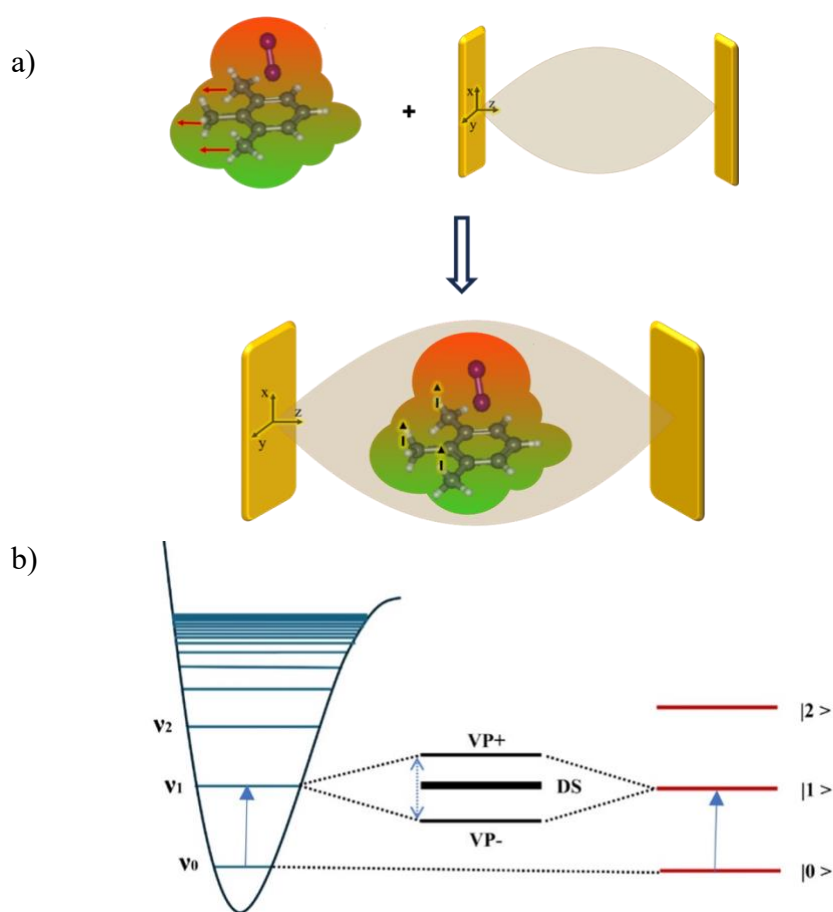


Figure 1. a) Sketch of vibrational strong coupling (VSC) of a cavity mode with a vibration of 1,2,3-trimethylbenzene of point group symmetry C_{2v} forming a CT complex with an acceptor molecule (I_2); the red arrows symbolize the A_1 mode of the methyl groups that is under VSC and black arrows symbolize the representation of the vibropolariton. The latter, as described in the text, is given by the direct product between the A_1 irreducible representation and those of the transverse field ($B_1(f)$ and $B_2(f)$) of the common

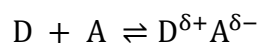
subgroup of the molecule and the cavity mode. The reaction coordinate is perpendicular to the aromatic ring towards I₂. b) Schematic representation of the strong coupling of a vibrational transition with an optical mode that gives rise to vibropolaritonic states, VP⁺, VP⁻ and dark states DS.

This selection in the vibrational symmetry either favored the product or not, relative to the normal uncoupled condition. At the same time, the underlying explanation for why it leads to a change in reactivity was not understood. In this Article, we extend the study on donor-acceptor charge transfer complexation by comparing three different isomers of tri-methyl-benzene of different symmetries with various acceptors. From the results emerges a phenomenological symmetry rule for the change in charge transfer chemistry and by extension, more generally for chemical reactivity under VSC.

Results and discussion:

The experiments were conducted both inside the cavity under VSC and outside the cavity as detailed in the SI. To achieve VSC for a selected vibrational mode, the cavity must be in resonance at normal incidence. It should be recalled that modification of molecular properties is only observed under such condition.^[19,20] Experimentally, the two vibro-polaritonic modes VP⁺ and VP⁻ can be seen in the IR spectrum as illustrated in Figure 2 a) when the vibrational band at 1378 cm⁻¹ of 123TMB (1,2,3 trimethylbenzene) is coupled.

Starting from stock solutions of donor and acceptor compounds, the acceptor A concentration was kept constant while that of the donor D was varied to extract the relevant data as follows. When a solution of D and A are mixed, they spontaneously form a charge transfer (CT) complex:



$$K_{DA} = \frac{[D^{\delta+}A^{\delta-}]}{[D][A]} = \frac{k_1}{k_{-1}} \quad \text{Eq. (1)}$$

DA complex has typically a new intense absorption CT band in the UV-Visible, as shown in Fig. 2b for iodine (acceptor) and 1,2,3 trimethylbenzene (donor), that can be monitored to determine

both the equilibrium constant (K_{DA}) and the absorption coefficient ε_{DA} of the complex by plotting the Benesi-Hildebrand equation (2) (Fig.2 d):^[55-60]

$$\frac{[A]_0}{Abs} = \frac{1}{\varepsilon_{DA}l} + \frac{1}{K_{DA}\varepsilon_{DA}l} \left(\frac{1}{[D]_0} \right) \quad \text{Eq. (2)}$$

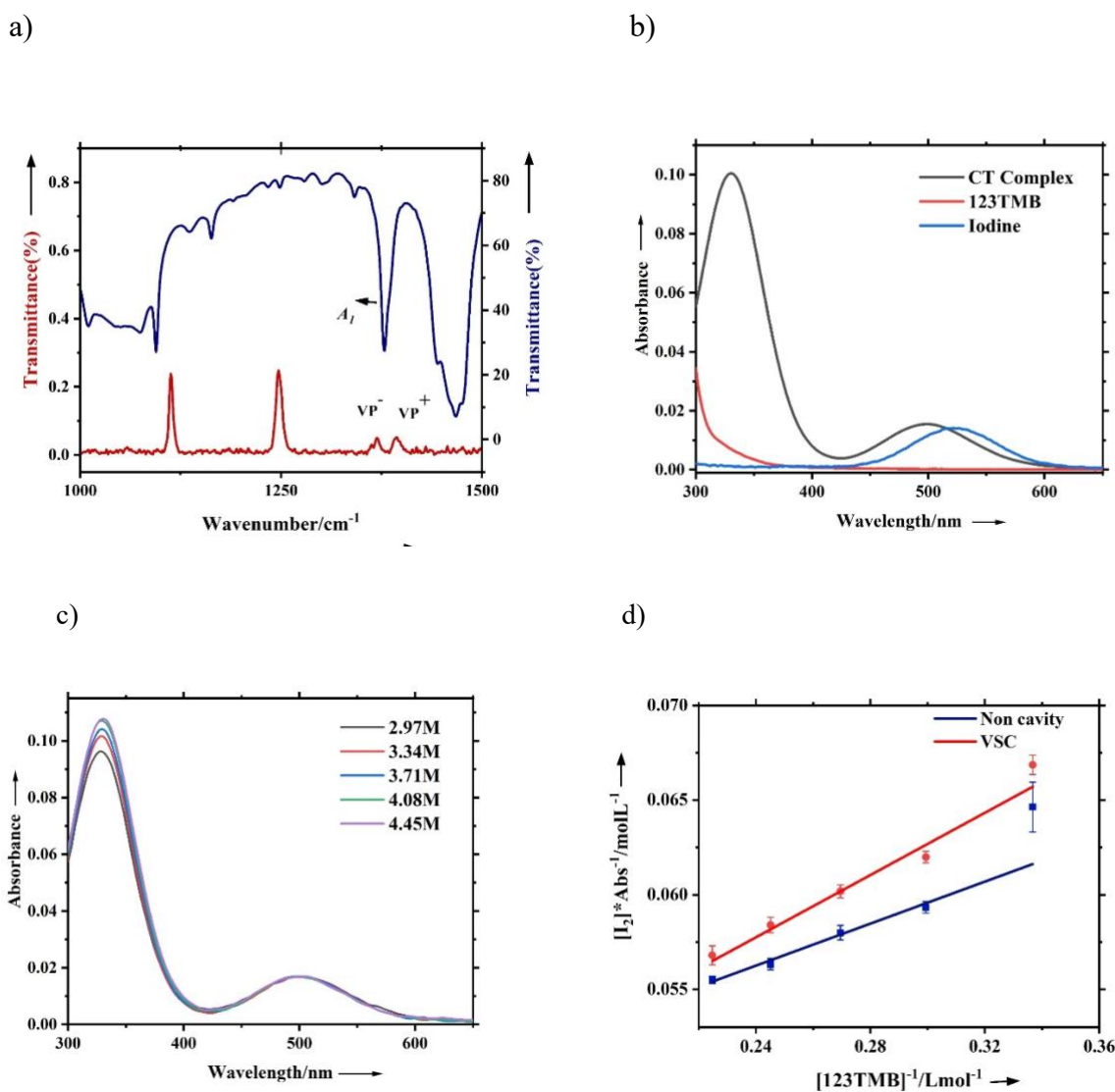


Figure 2. (a) IR spectra of 123TMB (donor D) – I₂ (acceptor A) CT complex (blue) with cavity mode (red) coupled with vibrational band of A₁ symmetry at 1378 cm⁻¹, (b) UV-VIS absorbance spectrum of the reactants and the CT complex in heptane, (c) evolution of the spectrum under VSC as a

function of [123TMB] in heptane and d) Benesi-Hildebrand plot under VSC and compared to that outside the cavity determined from the changes in absorbance of the CT complex at the maxima at 330 nm.

where the $[A]_0$ and $[D]_0$ are the initial concentrations of the acceptor and donor respectively, l corresponds to the path length, Abs corresponds to the absorbance of the CT complex for varying concentrations of the donor which is in excess compared to $[A]_0$. This protocol was used to analyze the consequences of VSC on the CT complexation by comparing it to the case outside the cavity as in Fig. 2 c) and d).

Tables 1, 2 and 3 summarize the results of our study of VSC of vibrational modes of different irreducible representations for various DA complexes, using for D three trimethylbenzene (TMB) isomers of different point group symmetry, namely 135, 123 and 124 TMB. Clearly, patterns can be seen in how VSC affects K_{DA} and ϵ_{DA} . While under normal conditions K_{DA} does not vary much for the three TMB isomers under complexation with I_2 (Table 1), the point group symmetry of the isomer impacts strongly the outcome of VSC experiments. For instance, upon coupling the 1378 cm^{-1} vibrational band ($-\text{CH}_3$ angular deformation mode), K_{DA} under VSC is found to be either unchanged, increased or decreased depending on the symmetry of the vibration of D. The absorption coefficient ϵ_{DA} is also found to change and this is most likely related to the relative position of A and D,^[17,60] but this will not be discussed further as it is outside the scope of this work.

Table 1: Complexation constants K_{DA} and absorption coefficients ϵ_{DA} of CT complexes of TMB isomers with I_2 , measured in heptane, outside the cavity and under VSC for vibrations associated with different irreducible representations (irr. rep.). Absorption coefficient ϵ_{DA} (320nm (124 TMB), 330nm (123 TMB/135 TMB) values are given in $10^4\text{ mol}^{-1}\text{ l cm}^{-1}$. # corresponds to the results for 135 TMB and I_2 taken from ref. 17. The point groups of the isomers are the global ones. The actual assignment of the irreducible representations for 135 TMB is based on the analysis in ref. 61 using local symmetry.

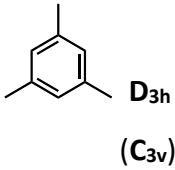
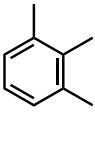
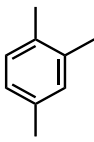
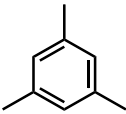
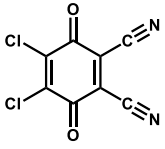
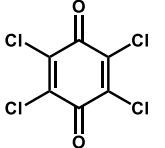
Acceptor	Donor	Outside the cavity		VSC		
		K_{DA}	ϵ_{DA}	Vibr. Bands (irr. rep.)	K_{DA}	ϵ_{DA}
I_2	135TMB # 	0.41±0.02	1.44±0.1	1378cm ⁻¹ (A')	0.15±0.02	4.70±0.5
	1468cm ⁻¹ (A')			0.16±0.02	3.63±0.4	
	1609cm ⁻¹ (E')			1.01±0.1	1.52±0.2	
	123TMB 	0.46±0.05	1.05±0.07	1378cm ⁻¹ (A ₁)	0.81±0.07	0.92±0.02
	1094cm ⁻¹ (A ₁)			0.80±0.11	0.95±0.05	
	124TMB 	0.57±0.02	0.89±0.01	1378cm ⁻¹ (A')	0.52±0.03	0.97±0.03
1507cm ⁻¹ (A')	0.31±0.03			1.18±0.09		

Table 2 compares the results of VSC for three different acceptors complexed with 135TMB. In all cases, an increase in K_{DA} by a factor of 1.5 to 3 is observed when an E symmetry band of the donor is directly coupled. For the bands of A and B_{1u} symmetry whether of the donor or acceptor, K_{DA} decreases to the same value within experimental error. It should be noted that in the case of 2,3-dichloro-5,6-dicyanobenzoquinone (DDQ), its A_1 band is cooperatively coupled with acetonitrile. In contrast, the K_{DA} of 124TMB - DDQ complex remains unchanged when the 2253 cm⁻¹ band (A_1 symmetry) is under VSC (Table S4) unlike the corresponding band for the 135TMB-DDQ complex (Table 2).

Table 2: Complexation constants K_{DA} and absorption coefficients ϵ_{DA} of 135TMB with different acceptors outside the cavity and under VSC for vibrations of both D and A and their irreducible representations (irr. rep.). ϵ_{DA} values are given in 10⁴ mol⁻¹ l cm⁻¹. # corresponds to the results for 135 TMB and I_2 measured in heptane from ref. 17. The experiment with chloranil and DDQ were carried out in acetonitrile. The point groups of the molecules are the formal ones. The actual

assignment of the irreducible representations for 135 TMB is based on the analysis in ref. 61 using local symmetry.

Donor	Acceptor	Outside the cavity		VSC					
		K_{DA}	ϵ_{DA}	D/A	Vibr. Band (irr. rep.)	K_{DA}	ϵ_{DA}		
 D_{3h} (C_{3v})	#	0.41±0.02	1.44±0.1	D	1378cm ⁻¹ (A')	0.15±0.02	4.70±0.5		
	I₂			D	1468cm ⁻¹ (A')			0.16±0.02	3.63±0.4
				D	1609cm ⁻¹ (E')			1.01±0.1	1.52±0.2
	 C_{2v}	D	0.26±0.01	0.68±0.02	D	1609cm ⁻¹ (E')	0.38±0.04	0.47±0.04	
		A			2253cm ⁻¹ (A ₁)	0.16±0.01			0.81±0.06
	 D_{2h}		0.23±0.02	0.30±0.01	A	905cm ⁻¹ (B _{1u})	0.14±0.01	0.48±0.01	
					D	1609cm ⁻¹ (E')			0.29±0.02

In these experiments under VSC, every coupling splits a vibrational peak into two, and therefore the vibrational degrees of freedom ν_f under VSC must increase and should be re-written as follows:

$$\nu_f = 3n - 6 + n_c \quad \text{Eq (4)}$$

where n_c corresponds to the sum of the vibrations V_c that are simultaneously coupled to the cavity times the number of Rabi splittings s per coupling so $n_c = \sum V_c (2s - 1)$. We recall that VSC can lead to more than one Rabi splitting as in ultra-strong coupling.^[29] In essence, the cavity brings n_c additional degrees of freedom to the coupled molecule and will thus affect the partition function. To apprehend the nature of these additional degrees of freedom, Mulliken's initial formulation of the CT complexation is inspiring^[55-59]. Mulliken describes the wavefunction of CT complexes by

the mixture of two states which define the representation basis set, a neutral DA pair and the ionic D^+A^- pair (ground and excited states):

$$\Psi_i(DA) = a\varphi_0(D, A) + b\varphi_1(D^+A^-)$$

$$\Psi_f(DA) = c\varphi_0(D, A) + d\varphi_1(D^+A^-)$$

where, $\varphi_0(D, A)$ is the non-bond wavefunction and $\varphi_1(D^+A^-)$ is the dative wavefunction and a, b, c, d are the mixing coefficients. These two states (φ_0, φ_1) are taken as basis wavefunctions for the complex wavefunction Ψ whose properties are entirely given by the mixing coefficients, i.e. the components of the complex wavefunction *projected* on this basis. These mixing coefficients depend on the orbital symmetries involved^[58] and must also be vibration symmetry dependent, in agreement with Bader^[6] who pointed out the importance of the vibrational symmetry in chemical reactivity. The significant change of the complexation constants under VSC must imply a modification of the degree of charge transfer in the complex reflecting in modified mixing coefficients (a, b, c , and d), manifesting the fact that the initial vibronic states have become vibropolaritonic states under VSC.

We boldly transpose this notion of *projection* into the realm of point group representations under VSC (i) by describing VSC as a selection of irreducible representations among a set given by the molecules and the cavity, and (ii) by using the fact that the CT complexation is spatially oriented along a reaction coordinate simply given by the direction of charge transfer between the donor and the acceptor (Fig. 3). This leads us to “*project*” in the way detailed below the selected irreducible representations with respect to the reaction coordinate. Each projection corresponds to a modification of the CT complexation paths with the two extreme cases of parallel vs. perpendicular projections expected to respectively enhance or reduce the CT reactivity.

In more detail, we first set the reference frame to represent the different point groups involved. In the context of VSC and longitudinal modes of the cavity at normal incidence with respect to the mirrors (with degenerate TE (transverse electric) vs. TM (transverse magnetic) modes), a natural frame is set by the intracavity optical mode with the longitudinal z-axis of the cavity (Fig.1a) and the transverse (x,y)-plane of the electric field polarization.

When reaching the strong coupling regime, the eigenstates of the system become hybridized, incorporating both light and matter components. This leads to a symmetry relation between both components which engages the common subgroups of both the molecular system

and the cavity. These common subgroups share a rotational symmetry axis (the cavity z-axis) within a unique spatial representation given by the transverse plane of polarization. From this shared representation, we then describe the overall symmetry associated with the hybridization from direct products performed within the set of irreducible representations of the common subgroups. To understand how the symmetry of the coupled vibration is modified by hybridization with the optical mode, and its chemical consequences, we first assign a point group to the electromagnetic mode in the cavity. We then see how the direct product of the mode representation with that of the molecular vibration leads to a new irreducible representation corresponding to the hybrid vibropolariton. Finally, since all irreducible representations are orthogonal, the resulting change in projection on the reaction coordinate is analyzed to explain the favorable or unfavorable modification in the charge transfer complexation reaction.

Let's take as a first example the case of 135TMB with I_2 under VSC.

Since the optical mode forms a standing wave along the z-axis (Fig. 1), degenerate in x and y, it can be analyzed in the $D_{\infty h}$ point group. The 135TMB isomer, strictly speaking of the D_{3h} point group, is typically assumed with the lower C_{3v} symmetry to explain the presence of the IR active bands such as CH_3 angular deformation mode.^[61] We choose the C_{3v} as the simplest common subgroup of the cavity and the molecule and we represent it within the frame set by the intracavity field. The corresponding character table for the C_{3v} common subgroup is given in Table 3.^[62]

Table 3: Character table for C_{3v} point group.

C_{3v}	E	$2C_3 (z)$	$3 \sigma_v$	
A_1	+1	+1	+1	z
A_2	+1	+1	-1	R_z
E	+2	-1	0	(x, y) (R_x, R_y)

From the character table, as per the explanation given above, the electric field f transforms as the E irreducible representation (noted as $E(f)$) being degenerate in x and y. Next we do the direct products of the representations $E(f)$ with A' (A' now A_1 in the subgroup) when vibration A' of the 135TMB is strongly coupled, or with E when vibration E of the 135TMB is strongly coupled. The

direct products can be reduced into $A_1 \otimes E(f) = E$ and the linear combination $E \otimes E(f) = A_1 \oplus A_2 \oplus E$, as shown in Table 4.

Table 4: Direct product of the irreducible representations

C_{3v}	E	$2C_3(z)$	$3\sigma_v$
$A_1 \otimes E(f) = E$	+2	-1	0
$E \otimes E(f) = A_1 \oplus A_2 \oplus E$	+4	1	0

This change in symmetry representation under VSC has immediate consequences. For the charge transfer complexation of 135TMB, when an A_1 symmetry vibration is coupled to the cavity mode, we see a decrease in K_{DA} (Table 1). This is because under VSC, the vibrational A_1 -symmetry state is changed into a vibropolariton that transforms as the E representation, as shown above by the direct product. Looking at the complexation, the reaction coordinate transforms as A_1 . The mode now in the E representation under VSC is now orthogonal with respect to the charge density displacement along the reaction coordinate of the CT complex. In other words, the projection of the vibropolariton on the reaction coordinate is null (Fig. 3). As a consequence, K_{DA} decreases.

On the contrary, when coupling the E symmetry vibration of 135TMB with the optical field, the CT complexation is favored. Here we see that the direct product of this vibration representation with the cavity mode ($E \otimes E(f)$) yields elements of the irreducible representations A_1 and A_2 to which correspond both the principal axis and the reaction coordinate of the charge transfer, explaining the increase in K_{DA} .

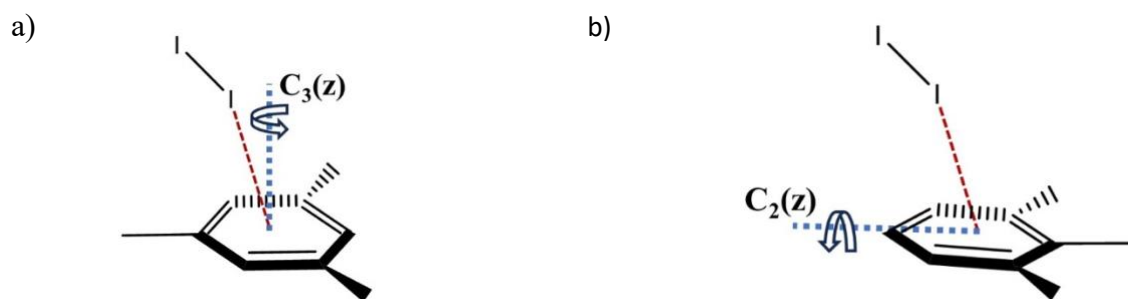


Figure 3. Illustration of the relationship of the principal axis (blue dotted line) of the molecule and the CT reaction coordinate (red dashed line) of a) 135TMB and b) 123TMB with I_2 .

Next let's consider the CT complexes of the 123TMB isomer with I_2 . The 123TMB isomer belongs to the point group C_{2v} and has its principal axis in the plane of the benzene ring, in other words orthogonal to the reaction coordinate as illustrated in Fig. 3b. As a consequence, we expect the opposite response to VSC as compared to 135TMB, as observed. The common subgroup with the optical field is also C_{2v} with the character Table 5.

Table 5: Character table for C_{2v} point group.

C_{2v}	E	$C_2(z)$	$\sigma_v(xz)$	$\sigma_v(yz)$	linear functions, rotations
A_1	+1	+1	+1	+1	z
A_2	+1	+1	-1	-1	R_z
B_1	+1	-1	+1	-1	x, R_y
B_2	+1	-1	-1	+1	y, R_x

In the C_{2v} subgroup, the cavity field transforms as the B_1 and B_2 irreducible representations, noted $B_1(f)$ and $B_2(f)$ representations along x and y. From the direct product in Table 6, the A_1 vibration now transforms as B_1 or B_2 both orthogonal to the principal axis C_2 , thus now along the charge transfer axis, i.e. its reaction coordinate (see Fig. 3b), leading to an increase in K_{DA} , as observed.

Table 6: Direct product of the irreducible representations

C_{2v}	E	$C_2(z)$	$\sigma_v(xz)$	$\sigma_v(yz)$
$A_1 \otimes B_1(f) = B_1$	+1	-1	+1	-1
$A_1 \otimes B_2(f) = B_2$	+1	-1	-1	+1

Finally, for the least symmetric isomer, 124TMB, the corresponding C_s point group has no well-defined principal axis. As a consequence, the changes under VSC are much smaller relative to the other two other isomers, consistent with the model.

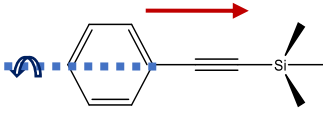
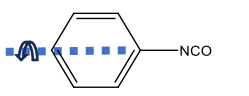
We can apply the same analysis to explain all the increases and decreases K_{DA} in Table 1 and 2 as shown in Table 7. In the latter, we have added results for a complex with two CT bands (spatial isomers) where the changes in the equilibrium constant can again be understood by the symmetry representation of the vibropolariton relative to the reaction coordinate. The modified K_{DA} under VSC reflect relative changes in the reaction rates of the charge transfer complexation (Eq. 1). Within the same symmetry-based approach, it should be possible to rationalize other modifications of reaction rates under VSC for instance, the silyl deprotection reaction reported in 2016 and more recently for alcoholysis reaction.^[21,31] These small molecule reactants have well defined symmetry and their reactions are well-known high-yield ones where most likely the vibronic overlap is already favorable.^[6] Therefore, it is not surprising that when VSC induces changes in symmetry representation of key vibrations so that they become orthogonal to the reaction coordinate, it decreases the rate as observed, reflecting a higher activation energy (see Table 7).

In summary, we have found a phenomenological link between chemical reactivity under VSC and symmetry representation. This link views VSC as generating a hybridization of a vibration and the optical field that results in a new irreducible representation for the vibropolariton, relative to the principal axis and thereby its projection on the reaction coordinate. Needless to say however that many other factors will also modify or obscure this rule. For instance, the vibrational states of the molecules are rarely pure normal modes so that the effect of vibrational symmetry changes will not always be detected, the more so the larger the molecules. VSC has to affect the limiting step in the pathway for it to be detectable in the rates although it could still be seen in the product yields in complex landscapes as already shown.^[22,36] Internal vibrational energy redistribution will also be affected by VSC as pointed out in recent theoretical studies.^[37-39] Furthermore, external conditions such as solvation can also influence the outcome.

While the molecules are randomly oriented, most molecules are coupled as shown in references 17 and 36 where phase transition like behavior is seen upon the onset of VSC, as there always some projection onto the field. Intermolecular interactions will further favor the coupling.

It is tempting to see whether the phenomenological symmetry principle identified here is also in agreement with other findings. For instance, recent results show that the conductivity of polystyrene can be boosted by 6 orders of magnitude when coupling the B_2 vibration of the styrene moiety.^[26] The B_2 vibration can only be changed under VSC to A_1 symmetry representation

Table 7: Summary of reactions under VSC and agreement with symmetry predictions: Reaction type (CT: charge transfer), point group of the molecule under VSC, irreducible representation of vibration in the common subgroup with the optical field, symmetry product, prediction and experimental observation.

Reaction	Point Group	Vibration irreducible represent.	Symmetry product with cavity mode	Prediction	Observation
135TMB → I ₂ CT	D _{3h} Donor	E (in C _{3v})	$E \otimes E(f) = A_1 + A_2 + E$	K_{DA} increases	K_{DA} increases for donor E symmetry vibrations
135TMB → DDQ CT					
135TMB → Chloranil CT					
135TMB → I ₂ CT	D _{3h} Donor	A ₁ (in C _{3v})	$A_1 \otimes E(f) = E$	K_{DA} decreases	K_{DA} decreases for donor E symmetry vibrations
123TMB → I ₂ CT	C _{2v} Donor	A ₁	$A_1 \otimes B_1(f) = B_1$ $A_1 \otimes B_2(f) = B_2$	K_{DA} increases	K_{DA} increases for donor E symmetry vibrations
135TMB → Chloranil CT	D _{2h} Acceptor	B ₁ (in C _{2v})	$B_1 \otimes B_1(f) = A_1$ $B_1 \otimes B_2(f) = A_2$	K_{DA} decreases	K_{DA} decreases for acceptor B _{1u} symmetry vibrations
Anisole → TCNE* CT 2 CT isomers	D _{2h} Acceptor	A ₁ (in C _{2v})	$A_1 \otimes B_1(f) = B_1$ $A_1 \otimes B_2(f) = B_2$	K_{DA} increases	K_{DA} increases for both CT complexes
Anisole → TCNE* CT 2 CT isomers	C _{2v} Donor	B ₂	$B_1 \otimes B_1(f) = A_1$ $B_1 \otimes B_2(f) = A_2$	K_{DA} decreases	K_{DA} decreases for isomer 1
Silyl deprotection ^[21] 	C _{2v}	A	$A_1 \otimes B_2(f) = B_2$ $A_1 \otimes B_1(f) = B_1$	Deceleration	Reaction rate decelerated
Alcoholysis of phenyl isocyanate ^[31] 	C _{2v}	A	$A_1 \otimes B_2(f) = B_2$ $A_1 \otimes B_1(f) = B_1$	Deceleration	Reaction rate decelerated

* A. Jayachandran, J. G. Ricca, M. Mahato, J. Wega, E. Vauthey, T.W. Ebbesen, in preparation

according to the C_{2v} symmetry of styrene, and thereby favoring the charge displacement along the principal axis of the styrene moiety. Of course, other factors are no doubt also involved such as the delocalized states associated with the collective coupling that contribute to boosting the conductivity.

Since the hybridization between the optical mode and the vibrations under VSC leads to novel combinations of irreducible representations, it is highly possible that electronic strong coupling (ESC) also results in symmetry changes in the electronic wavefunctions involved. This could lead to major changes in chemical landscapes, as observed for photochemical ones,^[63-66] since it would affect the mixing (configuration interaction) between the ground and excited states which define among other things the height of the reaction barrier.

Our results emphasize again the relevance of symmetry, and in particular vibrational symmetry, in chemical reactivity. Taken together with the fact that VSC induces no detectable changes in chemical shifts in the ^1H and ^{13}C NMR, in other words in the electronic density distribution in the molecules,^[36] it indicates that VSC acts primarily on the reaction pathways and not on the reactant electronic ground state. Thus, VSC is a unique tool to modify selectively vibrational symmetry and its projection on the reaction landscape. Such triggering of new mechanistic paths can also be combined with well demonstrated selective laser excitation of individual vibrations of reactants.^[8-16] By applying the symmetry rule identified here, it should be possible to help predict the outcome of reactions under VSC making it a useful a tool to manipulate and control reactions, and to understand their mechanism.

Conclusion:

While our phenomenological symmetry rule can account for many of the experimental findings, there is clear need for more theoretical work to understand many details. For instance, while the vibropolaritons, VP^+ and VP^- , are embedded in the new symmetry representation, their exact nature needs to be clarified. Furthermore, it has not escaped our attention that the origin of the normal incidence condition for seeing change in properties might be related to the fact the optical field symmetry breaks down at other angles.

Acknowledgements

We thank Vincent Robert and Giulio Ragazzon for careful reading and insightful comments. We also thank Tal Schwartz for fruitful discussions. We would also like to thank K. Joseph and S. Swaminathan for doing extra control experiments.

Funding Sources

We acknowledge the support of the International Center for Frontier Research in Chemistry (icFRC, Strasbourg), the Labex NIE projects (ANR-11-LABX-0058 NIE), and CSC (ANR-10-LABX-0026 CSC) within the Investissement d'Avenir program ANR-10-IDEX-0002-02. T.W.E. acknowledges the support of the ERC (project 788482 MOLUSC) and CG & TWE that of the ANR-24-RRII-0001 (project POLARITONIC).

References:

1. R.B. Woodward, R. Hoffmann, *Angew. Chem. Int. Ed.* **1969**, *8*, 781-853.
2. Kenichi Fukui, *Acc. Chem. Res.* **1971**, *4*, 57-64.
3. R. G. Pearson, *Comp. & Maths. with Appls.* **1986**, *12B*, 229-236.
4. E. Pollak, P. Pechukas *J. Am. Chem. Soc.* **1978**, *100*, 2984-2991.
5. W. F. Bailey, A. S. Monahan, *J. Chem. Ed.* **1978**, *55*, 489-493.
6. R. F. W. Bader, *Can. J. Chem.* **1962**, *40*(6), 1164-1175.
7. P.J. MacDougall, R.W.F. Bader, *J. Am. Chem. Soc.* **1985**, *107*, 6788-6795.
8. P.R. Hundt, M.E. van Reijzen, H. Ueta, R.D. Beck, *J. Phys. Chem. Lett.* **2014**, *5*, 1963-1967.
9. H. Frei, L. Fredin, G.C. Pimentel, *J. Chem. Phys.* **1981**, *74*, 397-411.
10. R.N. Zare, *Science* **1998**, *279*, 1875-1879.
11. Crim, F. Fleming, *Acc. Chem. Res.* **1999**, *32*, 877-884.
12. W. Zhang, H. Kawamata, K. Liu, *Science* **2009**, *325*, 203-306.
13. Z. Lin, C.M. Lawrence, D. Xiao, V.V. Kireev, S.S. Skourtis, J.L. Sessler, D.N. Beratan, I.V. Rubtsov, *J. Am. Chem. Soc.* **2009**, *131*, 18060-18062.
14. M. Delor, I.V. Sazeanovich, M. Towrie, J.A. Weinstein, *Acc. Chem. Res.* **2015**, *48*, 1131-1139.
15. A.A. Bakulin, R. Lovrincic, X. Yu, O. Selig, H.J. Bakker, Y.L.A. Rezus, P.K. Nayak, A. Fonari, V. Coropceanu, J.-L. Bredas, et al., *Nat. Commun.* **2015**, *6*, 7880.
16. J. G. Kim et al, *Nature* **2020**, *582*, 520-524.
17. Y. Pang, A. Thomas, K. Nagarajan, R. M. A. Vergauwe, K. Joseph, B. Patrahau, K. Wang, C. Genet, T. W. Ebbesen, *Angew. Chem. Int. Ed.* **2020**, *59*, 10436.

18. A. Sau, K. Nagarajan, B. Patrahau, L. Lethuillier-Karl, R. M. A. Vergauwe, A. Thomas, J. Moran, C. Genet, T. W. Ebbesen, *Angew. Chem. Int. Ed.* **2021**, *60*, 5712.
19. F. J. Garcia-Vidal, C. Ciuti, T. W. Ebbesen, *Science* **2021**, *373*, 6551.
20. K. Nagarajan, A. Thomas, T. W. Ebbesen, *J. Am. Chem. Soc.* **2021**, *143*, 16877–16889.
21. A. Thomas, J. George, A. Shalabney, M. Dryzhakov, S. J. Varma, J. Moran, T. Chervy, X. Zhong, E. Devaux, C. Genet, J. A. Hutchison, T. W. Ebbesen, *Angew. Chem. Int. Ed.* **2016**, *55*, 11462–11466
22. A. Thomas, L. Lethuillier-Karl, K. Nagarajan, R. M. A. Vergauwe, J. George, T. Chervy, A. Shalabney, E. Devaux, C. Genet, J. Moran, T. W. Ebbesen, *Science* **2019**, *363*, 615–619.
23. J. Lather, P. Bhatt, A. Thomas, T. W. Ebbesen, J. George, *Angew. Chem. Int. Ed.* **2019**, *58*, 10635
24. F. Verdelli, Y.-C. Wei, K. Joseph, M.S. Abdelkhalik, M. Goudarzi, S.H.C. Askes, A. Bazldi, E.W. Meijer, J. Gomez Rivas, *Angew. Chem. Int. Ed.* **2024**, *63*, e202409528.
25. J. Singh, J. Lather, J. George, *Chem Phys Chem* **2023**, *24*, e202300016
26. S. Kumar, S. Biswas, U. Rashid, K. S. Mony, G. Chandrasekharan, F. Mattiotti, R. M. A. Vergauwe, D. Hagenmuller, V. Kaliginedi, A. Thomas, *J. Am. Chem. Soc.* **2024**, *146*, 18999-19008.
27. K. Joseph, Bas de Waal, S. A. H. Jansen, J. J. B. van der Tol, G. Vantomme, and E. W. Meijer, *J. Am. Chem. Soc.* **2024**, *146*, 12130-12137.
28. K. Joseph, S. Kushida, E. Smarsly, E. Ihiwakrim, A. Thomas, G. L. Paravicini-Bagliani, K. Nagarajan, R. Vergauwe, E. Devaux, O. Ersen, U. H. F. Bunz, T.W. Ebbesen, *Angew. Chem., Int. Ed.* **2021**, *60* (36), 19665-19670.
29. J. George, T. Chervy, A. Shalabney, E. Devaux, H. Hiura, C. Genet, T.W. Ebbesen, *Phys. Rev. Lett.* **2016**, *117*, 153601.
30. C. Zhong, S. Hou, X. Zhao, J. Bai, Z. Wang, F. Gao, J. Guo, F. Zhang, *ACS Photonics* **2023**, *10*, 1618-1623.
31. W. Ahn, J. F. Triana, F. Recabal, F. Herrera, B. S. Simpkins, *Science* **2023**, *380*, 1165–1168.
32. K. Hirai, H. Ishikawa, Y. Takahashi, J. A. Hutchison, H. Uji-i, *Chem. – Eur. J.* **2022**, *28*, e202201260
33. T. Fukushima, S. Yoshimitsu, K. Murakoshi, *Chem. Sci.* **2023**, *14*, 11441–11446.
34. R. Damari, O. Weinberg, D. Krotkov, N. Demina, K. Akulov, A. Golombek, T. Schwartz, S. Fleischer, *Nat. Commun.* **2019**, *10*, 3248.
35. G. Stemo, H. Yamada, H. Katsuki, H. Yanagi, *J. Phys. Chem. B* **2022**, *126*, 9399–9407.
36. B. Patrahau, M. Piejko, R.J. Mayer, C. antheaume, T. Sangchai, G. Ragazzon, A. Jayachandran, E. Devaux, C. Genet, J. Moran, T.W. Ebbesen, *Angew. Chem. Int. Ed.* **2024**, *63*, e202401368.
37. C. Schäfer, J. Flick, E. Ronca, P. Narang, A. Rubio, *Nat. Commun.* **2022**, *13*, 7817.
38. J. Sun, O. Vendrell, *J. Phys. Chem. Lett.* **2022**, *13*, 4441-4446.
39. S. Mondal, S. Keshavamurthy, *J. Chem. Phys.* **2024**, *161*, 194302.
40. L.P. Lindoy, A. Mandal, D.R. Reichman, *Nat. Commun.* **2023**, *14*, 2733.
41. D.S. Wang, T. Neuman, S.F. Yelin, J. Flick, *J. Phys. Chem. Lett.* **2022**, *13*, 3317-3324.

42. M.R. Fiechter, J.E. Runeso, J.E. Lawrence, J.O. Richardson, *J. Phys. Chem. Lett.* **2023**, *14*, 8261-8267.
43. K. Sun, R.F. Ribeiro, *Nat. Commun.* **2024**, *15*, 2405.
44. M. R. Fiechter, J.O. Richardson, *J. Chem. Phys.* **2024**, *160*, 184107.
45. Q. Yu, J.M. Bowman, *Nat. Commun.* **2023**, *14*, 3527.
46. P.-Y. Yang, J. Cao, *J. Phys. Chem. Lett.* **2021**, *12*, 9531–9538.
47. T. E. Li, A. Nitzan, J. E. Subotnik, *J. Chem. Phys.* **2020**, *152*, 234107.
48. D. Sidler, M. Ruggenthaler, C. Schäfer, E. Ronca, A. Rubio, *J. Chem. Phys.* **2022**, *156*, 230901
49. M. Castagnola, T.S. Haugland, E. Ronca, H. Koch, C. Schäfer, *J. Phys. Chem. Lett.* **2024**, *15*, 1428-1434.
50. M. Sukharev, J. Subotnik, A. Nitzan, *J. Chem. Phys.* **2023**, *158*, 084104.
51. J. Fregoni, F. J. Garcia-Vidal, J. Feist, *ACS Photonics* **2022**, *9*, 1096–1107.
52. J. Cao, E. Pollak, **2023**, DOI 10.48550/arXiv.2310.12881.
53. B.M. Weight, D.J. Weix, Z.T. Tonzetich, T.D. Krauss, P. Huo, *J. Am. Chem. Soc.* **2024**, *146*, 16184-16193.
54. G. D. Scholes, C. A. DelPo, B. Kudisch, *J. Phys. Chem. Lett.* **2020**, *11*, 6389–6395
55. H. A. Benesi, J. H. Hildebrand, *J. Am. Chem. Soc.* **1949**, *71*, 2703–2707.
56. R. S. Mulliken, *J. Am. Chem. Soc.* **1952**, *74* (3), 811-82.
57. R. S. Mulliken, W. B. Person, *Annu. Rev. Phys. Chem.* **1962**, *13*, 107–126.
58. C.J. Bender, *Chem. Soc. Rev.* **1986**, *15*, 475-502.
59. C. Kendrow, J. C. Baum, C. J. Marzocco, *J. Chem. Educ.* **2009**, *86*, 1330-1334.
60. F.C. Grozema, R.W.J. Zijlstra, M. Swart, P.T. van Duijnen, *Int. J. Quantum Chem.* **1999**, *75*, 709-723.
61. B.V. Lokshin, V.T. Aleksanyan, M.G. Ezernitskaya, *Russ. Chem. Bull.* **31**, 1995-1999 (1982).
62. F.A. Cotton, "Chemical Applications of Group Theory, Wiley-Interscience, New York, 1971
63. J. A. Hutchison, T. Schwartz, C. Genet, E. Devaux, T.W. Ebbesen, *Angew. Chem. Int. Ed.* **2012**, *51*, 1592–1596.
64. J. Mony, C. Climent, A.U. Petersen, K. Moth-Poulsen, J. Feist, K. Börjesson, *Adv. Funct. Mater.* **2021**, *31*, 2010737.
65. R. Puro, J.D.B Van Schenck, R.Center, E.K. Holland, J.E. Anthony, O. Ostroverkhova, *J. Phys. Chem. C* **2021**, *125*, 27072–27083.
66. H. Zeng, J.B. Pérez-Sanchez, C.T. Eckdahl, P. Liu, W.J. Chang, E.A. Weiss, J.A. Kalow, J. Yuen-Zhou, N.P. Stern, *J. Am. Chem. Soc.* **2023**, *145*, 19655-19661.

TOC: A general symmetry rule emerges from the study of charge transfer complexes in cavities that points to an underlying framework to predict the outcome of chemical reactivity under vibrational strong coupling.

